A Basic Study on Nonlinear Sound Propagation by Finite Element Simulation

Takao TSUCHIYA* and Yukio KAGAWA**

SYNOPSIS

A finite element approach to the calculation of nonlinear sound propagation is proposed. Under the assumption of a weak nonlinearity, a linearized one-dimensional equation is considered. The equation is discretized in space, and is then solved for time by using Newmark-β integration scheme, in which a numerical damping is devised. Some numerical demonstrations are made for the nonlinear sound propagation of a single-shot pulse in air. It is shown that the shock wave propagation is stably and accurately simulated by the introduction of the numerical damping.

1. Introduction

A parametric acoustic array and a shock wave are some of the interesting examples in sound waves of nonlinearity. These phenomena are mainly caused from the nonlinear waveform distortion as sound speed depends on the sound pressure. It is, therefore, important to analyze the waveform distortion in nonlinear sound waves.

There are two main methods to calculate the acoustic nonlinear distortion. One is a time domain method and the other is a frequency domain method. In the time domain method, the waveform distortion is calculated as a sound wave progresses over a small spatial interval in the time domain. A finite difference method[1] is known as a typical numerical approach to the time domain method as it is widely used to solve general differential equations. It has an advantage of providing direct discretization capability,

---

* Graduate School of Natural Science and Technology

** Department of Electrical and Electronic Engineering

but hard to cope with a field of arbitrary boundary shape. Another numerical method for time domain[2,3] is the method in which the waveform is geometrically calculated. In this method, the waveform distortion of a plane wave can easily be obtained without solving the wave equation because the changes in the pressure waveform are geometrically calculated simply by taking the dependence of sound speed on the sound pressure into account. It cannot be used for two or three-dimensional problems because it does not include the diffraction effect. On the other hand, the frequency domain method[4,5] uses a Fourier analysis. In the frequency domain method, the waveform is expanded into a Fourier series and a set of coupled wave equations are numerically solved for each frequency components. Then the waveform is obtained by the inverse Fourier transformation. Three-dimensional problems can easily be solved by the frequency domain method with which it is however difficult to include reflecting or scattering boundary conditions.

This paper proposes another numerical approach to calculate the nonlinear sound propagation by means of finite element method[6]. The present finite element method is a time domain method which can cope with the cases of heterogeneous medium and with reflecting or scattering boundaries of arbitrary shape. In this paper, one-dimensional cases are only considered for investigating the fundamental behavior. Kuznetsov's equation[7] is used as the governing equation of a nonlinear sound propagation. It is discretized by finite element method in space and then solved for time using Newmark-β integration scheme[8] in which a numerical damping is devised. Some numerical demonstrations are made for both linear and nonlinear sound propagation in air for which numerical error is examined.

2. Governing equation

We here consider the nonlinear sound propagation in a homogeneous fluid under the assumption that shock waves may occur but weakly during the course of sound propagation. The nonlinear sound wave is governed by the following Kuznetsov's equation:

$$\left(1 + \frac{\delta}{c_0^2}\frac{\partial}{\partial t}\right)\nabla^2\phi - \frac{1}{c_0^2}\frac{\partial^2\phi}{\partial t^2} = -\frac{1}{c_0^2}\frac{\partial}{\partial t}\left[(\nabla\phi)^2 + \frac{B/A}{2c_0^2}\left(\frac{\partial\phi}{\partial t}\right)^2\right] \qquad (1)$$

where ϕ is velocity potential, c_0 sound speed of small amplitude wave, t time, B/A nonlinearity parameter of the medium, and δ sound diffusibility due to viscosity and thermal conductivity of the medium. The right hand side of eq.(1) expresses the sound nonlinearity. It acts as a virtual and spatial driving term which causes the waveform distortion[9]. It consists of two terms: one associated with the particle velocity and the other with the sound pressure. Both nonlinear terms contribute to the waveform distortion but differently since the distribution of the particle velocity is not the same as that of the sound pressure due to the diffraction effect. For an example, in a non-

collinear interaction between two waves consisting of high and low frequencies, the contribution of each term was changeable as the effective nonlinearity parameter depended on the interaction angle between the two waves, which we previously reported[10].

Here we consider a plane wave propagating to x-direction. The one-dimensional governing equation is written as

$$\left(1+\frac{\delta}{c_0^2}\frac{\partial}{\partial t}\right)\frac{\partial^2\phi}{\partial x^2}-\frac{1}{c_0^2}\frac{\partial^2\phi}{\partial t^2}=-\frac{1}{c_0^2\partial t}\left[\left(\frac{\partial\phi}{\partial x}\right)^2+\frac{B/A}{2c_0^2}\left(\frac{\partial\phi}{\partial t}\right)^2\right] \qquad (2)$$

In the analytical procedure that is usually practiced for a progressive plane wave problem, under the assumption of the linear impedance relation, eq.(2) is written as

$$\left(1+\frac{\delta}{c_0^2}\frac{\partial}{\partial t}\right)\frac{\partial^2\phi}{\partial x^2}-\frac{1}{c_0^2}\frac{\partial^2\phi}{\partial t^2}=-\frac{1+B/2A}{c_0^4}\frac{\partial}{\partial t}\left(\frac{\partial\phi}{\partial t}\right)^2 \qquad (3)$$

which is known as Westervelt's equation[11]. This equation is only correct for a progressive plane wave. However, it cannot be used for a field which has discontinuity, at which wave is reflected so that the incident interacts with the reflected. The superposition of the two waves cannot simply be made as the waveform of the sound pressure is not the same as that of the particle velocity, so that a linear impedance relation does not hold for this case. Therefore eq.(3) does not express the nonlinear phenomenon exactly at the reflection point. Even in one-dimensional cases, it is necessary to take into account both nonlinear terms associated with the particle velocity and the sound pressure for exact analysis[12].

Observing a waveform on the coordinate which moves to positive x-direction at sound speed c_0, eq.(3) is rewritten as

$$\frac{\partial\phi}{\partial\tau}-\frac{1+B/2A}{2}\left(\frac{\partial\phi}{\partial\xi}\right)^2=\frac{\delta}{2}\frac{\partial^2\phi}{\partial\xi^2} \qquad (4)$$

where

$$\xi = x - c_0 t$$

and

$$\tau = t.$$

Equation(4) is a Burgers' equation which is known to give a weak shock solution[13]. The shock formation distance x_s is given by eq.(4) for angular frequency ω as[2]

$$x_s = \frac{\rho_0 c_0^3}{(1+B/2A)\omega P} \qquad (5)$$

where ρ_0 is medium density and P sound pressure.

3. Spatial discretization by finite element method

Now we are to solve eq.(2) numerically. The equation is discretized in space by a Galerkin's method. The one-dimensional region to be analyzed is divided into line elements for which the third order polynomial is used for test function. The discretized equation have the following form:

$$[M]\{\ddot{\phi}\} + [R]\{\dot{\phi}\} + [K]\{\phi\} = \{F\} + \{V\} \qquad (6)$$

where $\{\phi\}$ is the nodal velocity potential vector, $[M]$, $[R]$ and $[K]$ are mass, damping and stiffness matrices, $\{F\}$ is the driving source vector and the dot indicates the derivative with respect to time. $\{V\}$ is the nonlinear driving vector corresponding to the virtual source and it consists of two terms as

$$\{V\} = \{V_u\} + \{V_p\} \qquad (7)$$

where $\{V_u\}$ and $\{V_p\}$ are the virtual source vectors associated with the particle velocity and that with the sound pressure, respectively.

Equation(6) is then solved for time using the Newmark-β scheme[8]. In the present procedure, the equation of motion (eq.(6)) at a discrete time $t+\Delta t$ is written as

$$[M]\{\ddot{\phi}_{t+\Delta t}\} + [R]\{\dot{\phi}_{t+\Delta t}\} + [K]\{\phi_{t+\Delta t}\} = \{F_{t+\Delta t}\} + \{V_{t+\Delta t}\} \qquad (8)$$

where

$$\{\phi_{t+\Delta t}\} = \{\phi_t\} + \Delta t\{\dot{\phi}_t\} + \Delta t^2\Big[(0.5 - \beta)\{\ddot{\phi}_t\} + \beta\{\ddot{\phi}_{t+\Delta t}\}\Big] \qquad (9)$$

$$\{\dot{\phi}_{t+\Delta t}\} = \{\dot{\phi}_t\} + \Delta t\Big[(0.5-v)\{\ddot{\phi}_t\} + (0.5+v)\{\ddot{\phi}_{t+\Delta t}\}\Big] \qquad (10)$$

β is a parameter ($0<\beta<0.5$), v is a parameter to provide a numerical damping and Δt is time step. Substituting eqs.(9) and (10) into eq.(8), we obtain the motional response after a travelling of time Δt as

$$\{\ddot{\phi}_{t+\Delta t}\} = [Z]^{-1} (\{F_{t+\Delta t}\} + \{V_{t+\Delta t}\} - [R]\{A\} - [K]\{B\}) \qquad (11)$$

where

$$[Z] = \{[M] + (0.5 + v)\Delta t[R] + \beta \Delta t^2[K]\} \qquad (12)$$

$$\{A\} = \{\dot{\phi}_t\} + (0.5 - v)\Delta t\{\ddot{\phi}_t\} \qquad (13)$$

$$\{B\} = \{\phi_t\} + \Delta t\{\dot{\phi}_t\} + (0.5 - \beta)\Delta t^2\{\ddot{\phi}_t\} \qquad (14)$$

Substituting eq.(11) into eqs.(9) and (10), we then obtain the response at time $t+\Delta t$ from the response at time t.

It is known in time dependent problems that errors due to the higher order fluctuation often lead to unstable solution of rapid spatial fluctuation. For the calculation of a shock wave propagation, the errors due to the higher order terms

degrade the accuracy of a solution. There are some remedy to reduce the errors. We here introduce a numerical damping[14] into the Newmark-β time integration scheme. The numerical damping is an artificial damping which performs the same operation as that of a low-pass filter. Therefore, using this device, the solution for relatively low frequency region can accurately be obtained. The calculation accuracy is however degraded in the same frequency region as the errors present. In the Newmark-β scheme, the degree of the numerical damping corresponds to the value v ($v>0$) for which as the value of v increases, the damping increases. It is necessary to chose a suitable value of v depending on problems.

The calculation procedure is made in such a way that matrices $[M]$, $[R]$ and $[K]$ are first calculated and initial values are assigned to vectors $\{\phi_t\}$, $\{\dot{\phi}_t\}$, $\{\ddot{\phi}_t\}$ and $\{F_t\}$. Then the potential vectors $\{\phi_{t+\Delta t}\}$, $\{\dot{\phi}_{t+\Delta t}\}$ and $\{\ddot{\phi}_{t+\Delta t}\}$, the responses after a travelling of time Δt, are calculated. Finally, the virtual driving vector $\{V_{t+\Delta t}\}$ is calculated. In the next step, the driving vector is now set to $\{F_{t+\Delta t}\}+\{V_{t+\Delta t}\}$ and the responses after another step Δt are solved. This process is repeated.

4. Numerical examples

4.1 Field model

The one-dimensional field model is shown in Fig.1. The sound propagation in air is demonstrated for a single-shot pulse. The field to be analyzed is divided into line elements of the third order. The element length Δl is chosen in the range of $\lambda/40$ to $\lambda/100$ where λ is wavelength, and the time step Δt is chosen in the range of $T/1000$ to $T/4000$, where T is pulse width. To reduce CPU time for calculation, a frame technique is used for long distance propagation in such a way that a framed region is shifted to the x-direction as the pulse propagates and the calculation is only made for the region where the pulse exists.

The finite element solution of the linear wave propagation is compared with the exact solution to check the accuracy. For the nonlinear case, the analytical solution[15] for Burgers' equation is used for error estimation. Numerical calculations are performed in double precision on super computer (NEC SX-1E).
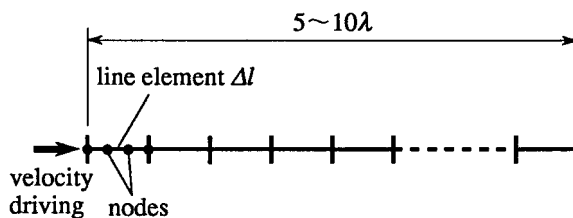

Fig.1 One-dimensional field model (the third order elements).
medium : air (ρ_0=1.2kg/m³, c_0=340m/sec)

4.2 Linear propagation

To check the validity of our program developed, the propagation of the sound in a small amplitude is first simulated. Figure 2 shows the changes of the pressure waveform as the wave of the amplitude of 1Pa progresses until the time $100T$. Figure a) and b) is the finite element solutions without numerical damping ($\nu=0$) and with ($\nu=0.06$). In this calculation, the element length is chosen to be $\lambda/70$, the time step $T/2000$, and $\beta=0.3025$. The nonlinear distortion does not appear with this amplitude and the pulse linearly propagates as it is. The solutions are accurately calculated without special care. The amplitude damps in the presence of the numerical damping as the pulse propagates. Figure 3 shows a relation between the propagation distance and the calculation error at the peak of the pulse. In the figure, circles and dots indicate the errors without and with the numerical damping. The solutions without the numerical damping provide the results of the error less than 1% at each wavelength distance. The effect of the numerical damping on the frequency characteristics (Fourier transform) which is calculated at the distance 100λ away from the sound source is shown in Fig.4. It shows that the numerical damping causes the same effect as the one of a low-pass filter. Figure 5 shows a relation between the damping parameter ν and the calculation errors in peak pressure at the same point. As the value ν increases, the amplitude decreases. As the results, the accurate solution is obtained without the numerical damping for the linear problem.
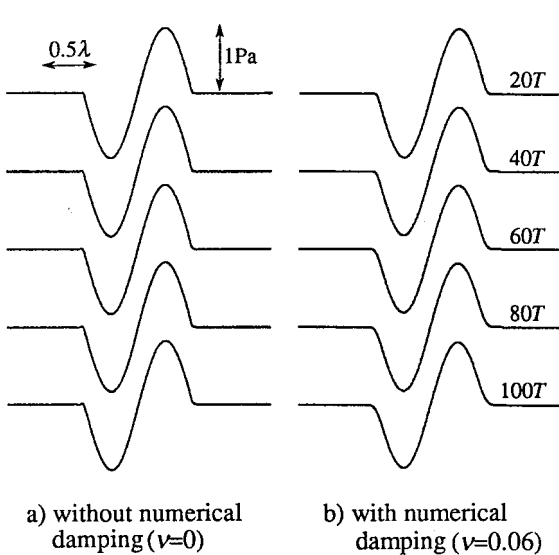

a) without numerical
   damping ($\nu=0$)

b) with numerical
   damping ($\nu=0.06$)

Fig.2 Finite element solutions for linear wave
propagation of a single-shot pulse.
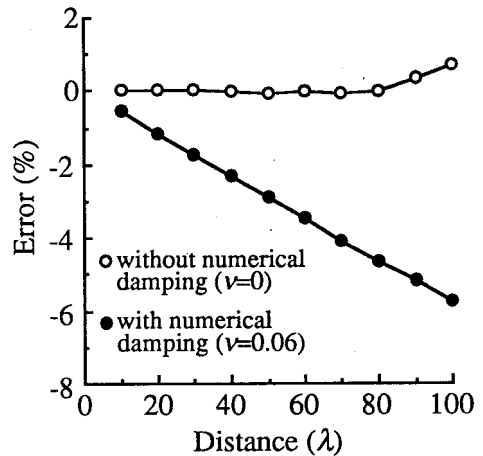(P=1Pa, $\Delta l=\lambda/70$, $\Delta t=T/2000$, $\beta=0.3025$)

Fig.3 Relation between the propagation
distance and the calculation error
at peak pressure.
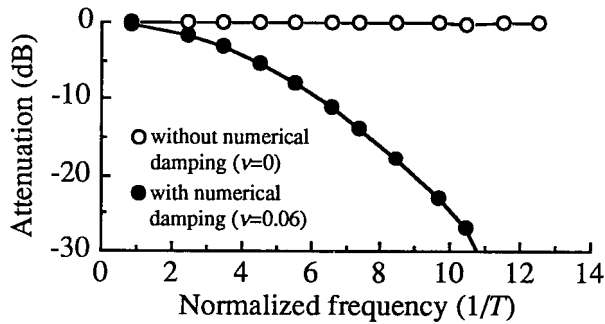($\Delta l=\lambda/70$, $\Delta t=T/2000$, $\beta=0.3025$)

Fig.4 Frequency spectrum change due to the presence
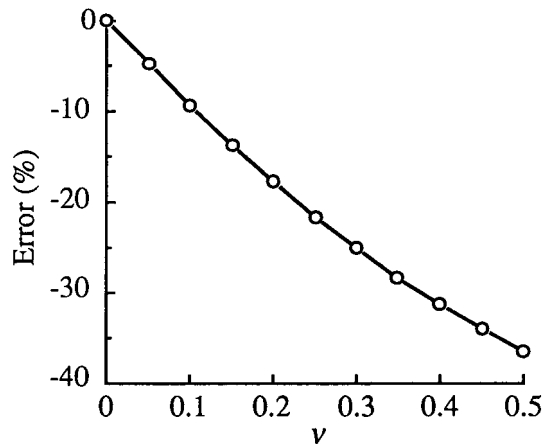of the numerical damping. (at $x=100\lambda$)

Fig.5 Relation between the damping parameter v and
the calculation error at peak pressure. (at $x=100\lambda$)

4.3 Nonlinear propagation

4.3.1 Nonlinear propagation of a single-shot pulse

Next, the nonlinear sound propagation of a single-shot pulse is simulated for the sound of amplitude 1kPa. The shock formation distance x_s becomes 18.4λ for this amplitude. Figure 6 shows the changes in the pressure waveform up to the time $50T$. Figure a) and b) are the finite element solutions without and with the numerical damping, respectively, and c) is the analytical solutions. Other parameters are the same as in the previous linear analysis (Fig.2) except that Δt is chosen to be $T/5000$ in the figure a) because the solution diverges for $\Delta t=T/2000$. The solutions are not stable without the numerical damping as shown in figure a) but its introduction is capable of eliminating this fluctuation as shown in figure in b). The finite element solutions with
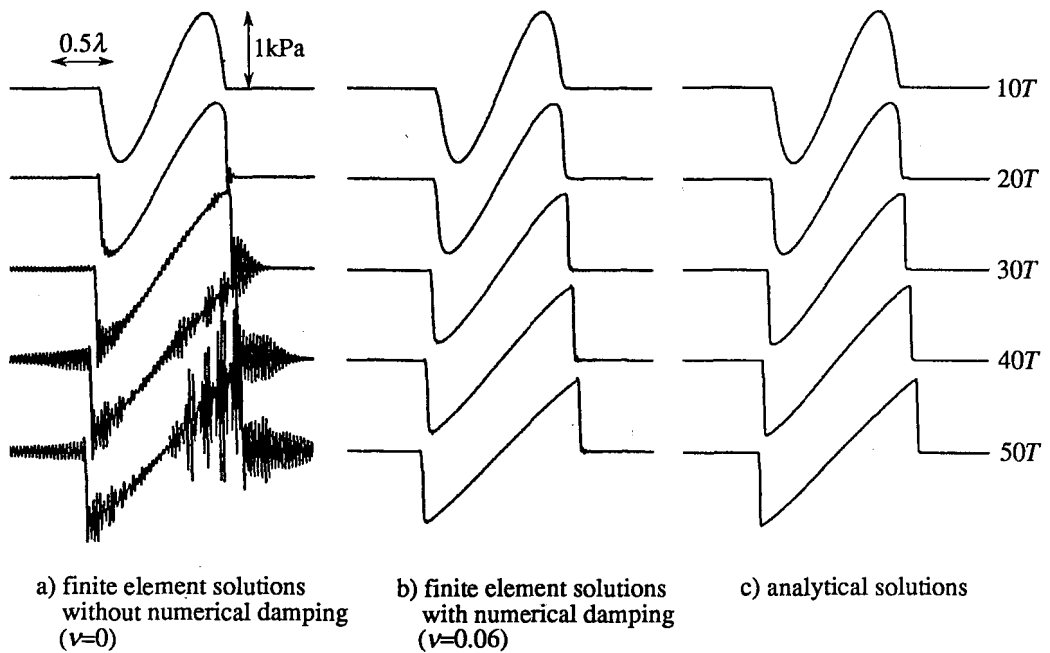
a) finite element solutions
without numerical damping
(ν=0)

b) finite element solutions
with numerical damping
(ν=0.06)

c) analytical solutions

Fig.6 Nonlinear wave propagation of a single-shot pulse.
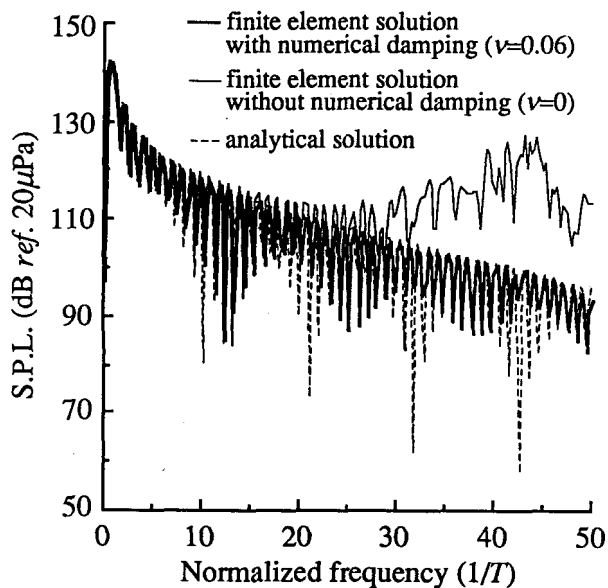(P=1kPa, Δl=λ/70, Δt=T/2000, β=0.3025)

Fig.7 Frequency spectrum of the shock wave.
(x=50λ, Δl=λ/70, Δt=T/2000, β=0.3025)

the numerical damping well agree with the analytical solutions. Figure 7 shows the
frequency spectrum of the pressure waveform calculated at the distance 50λ away from

the sound source. In the figure, fine and bold lines indicate the finite element solutions without and with the numerical damping, respectively and dashed lines indicate the analytical solutions. The error increases in the high frequency region without the numerical damping. As the numerical damping is thus devised in the time domain, the finite element solutions give reasonable results over the wide frequency range. Nonlinear sound propagation can be calculated with reasonable accuracy by devising the numerical damping.

4.3.2 Effect of the numerical damping

We here investigate a relation of the parameter of the numerical damping v on the solution accuracy more in detail. Figure 8 shows the changes in the pressure waveform whose amplitude is increased to 5kPa. Other parameters are the same as in the previous nonlinear analysis given in Fig.6 b). As the amplitude is increased to 5kPa, the fluctuation again appears in the solutions. This is due to the fact that the time integration for interval Δt cannot properly follow this intense amplitude because the waveform change is more rapid for the wave of large amplitude than that of small amplitude. This means that a suitable value must be chosen for v according to the pressure. Figure 9 shows the relation between the sound pressure and the suitable range for the value of v. In the figure, broken and solid lines indicate the case that a sound wave propagates over 2 or 10 times longer distance than the shock formation distance x_s, respectively and $\bigcirc$ and $\triangle$ indicate the lower bounds of v, and $\bullet$ and $\blacktriangle$ the upper bounds for the allowance of 1dB error. In smaller amplitude, the value v comes close to 0 because the sound
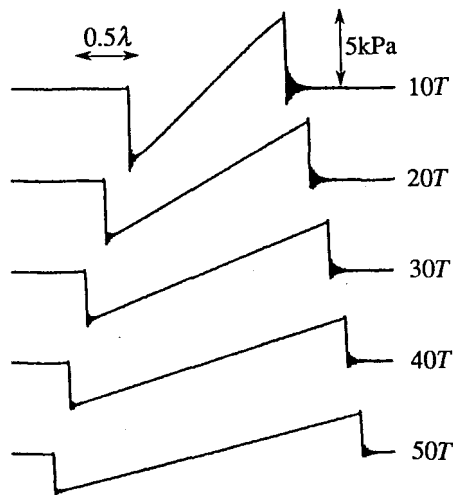

Fig.8 Nonlinear pulse wave propagation of large amplitude.
(P=5kPa, $\Delta l=\lambda/70$, $\Delta t=T/2000$, β=0.3025, v=0.06)
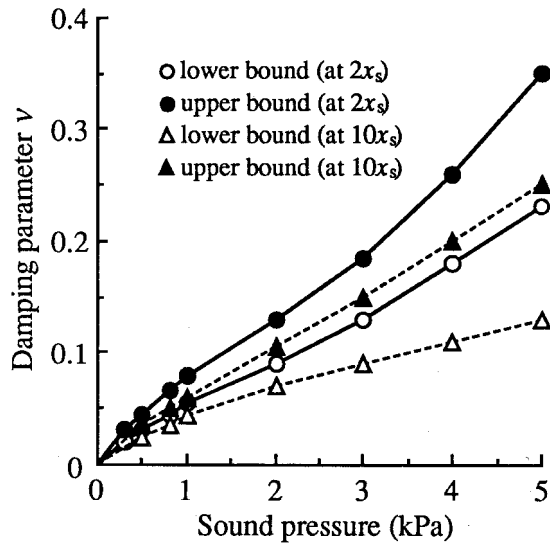
Fig.9 Relation between the sound pressure and suitable
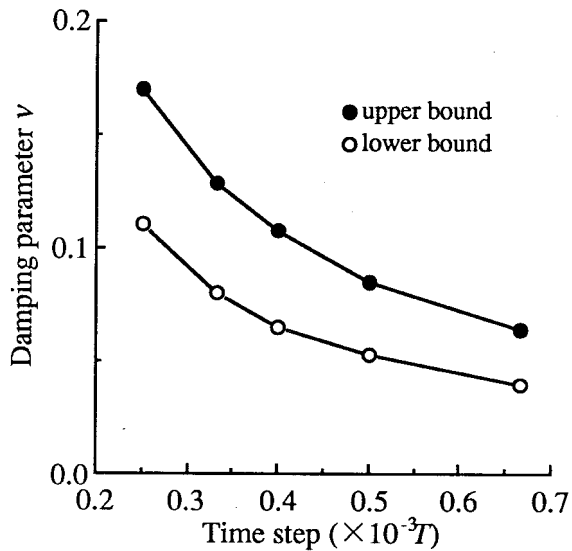damping parameter for 1dB error allowance.

Fig.10 Relation between the time step and suitable
damping parameter for 1dB error allowance.
($x=2x_s$, $P=$1kPa)

wave is almost linear, while larger value must be taken for larger amplitude. The
suitable value of v can be smaller as the pulse propagates over a long distance as
expected because the amplitude decreases due to the nonlinear absorption. The
acceptable range of v becomes narrower and is more sensitive to the amplitude for
smaller amplitude.

Figure 10 shows a relation between the time step Δt and the value of v for suitable solutions. The amplitude is chosen to be 1kPa and the propagation distance $2x_s$. The suitable value of v is inversely proportional to time step Δt. This is because the cut-off frequency of the numerical damping as the filter is given as a reciprocal of Δt. The present numerical experiment shows that suitable value of Δt is chosen in the range of 0.25×10^{-3}-1×10^{-3} for the accurate shock calculation.

In time dependent problems, it is known that the calculation accuracy depends on both element length Δl and time step Δt. To evaluate this dependence, a following parameter is often introduced:

$$\kappa = 3c_0\Delta t/\Delta l \qquad\qquad (15)$$

Values of κ corresponding to the case of Fig.10 are 0.05-0.21. Though the parameter κ thus depends on the element length Δl, our numerical experiment shows that the parameter v does not depend on Δl. The element length Δl must be less than $\lambda/40$ to hold reasonable accuracy.

5. Concluding remarks

A numerical approach to the calculation of a nonlinear sound wave propagation by finite element method is proposed. Only a plane sound wave is considered. It is shown that the nonlinear sound propagation can be calculated up to the formation of the shock waves with reasonable accuracy. Newmark-β time integration scheme is used devising the numerical damping. Some numerical experiments are carried out for the propagation of a single-shot pulse and the relation of the numerical damping on the calculation accuracy is examined. It is found that for accurate shock wave simulation the element length must be less than $\lambda/40$ and the time step must be chosen less than $T/1000$. Though only one-dimensional cases are demonstrated in the present paper, it is straightforward to expand this method into two or three-dimensional cases.

References

1) A.Harten; "High resolution schemes for hyperbolic conservation laws," J. Comp. Phys. **49**, pp.357-393 (1983).

2) F.M.Pestorius; "Propagation of plane acoustic noise of finite amplitude," Technical Report **ARL-TR-73-23**, Applied Research Laboratories, The Univ. of Texas at Austin, (1973).

3) Y.Watanabe and Y.Urabe; "Experiments and algorithm of calculation concerning the propagation of finite amplitude waves -Nonlinear acoustics(3)-," J. Acoust. Soc. Jpn. **38**, pp.105-112 (1982). [*in japanese*]

4) S.I.Aanonsen, T.Barkve, J.N.Tjøtta and S.Tjøtta; "Distortion and harmonic generation in the nearfield of a finite amplitude sound beam," J. Acoust. Soc. Am. **75**, pp. 749-768 (1983).

5) T.Kamakura, I.Abiru and Y.Kumamoto; "Nonlinearity generated waveform distortion of ultrasonic pulses," J. Acoust. Soc. Jpn. **46**, pp.802-809 (1990). [*in japanese*]

6) T.Tsuchiya and Y.Kagawa; "Simulation of nonlinear sound propagation by finite element method," IEICE Technical Report **US90**-64, pp17-24 (1991). [*in japanese*]

7) V.P.Kuznetsov; "Equations of nonlinear acoustics," Sov. Phys. Acoust. **16**, pp.467-470 (1971).

8) N.M.Newmark; "A method for computation of structural dynamics," Proc., ASCE, J. Eng. Mech. Div., **85-EM** 3, pp.467-470 (1971).

9) T.Tsuchiya, Y.Watanabe and Y.Urabe; "Theoretical approach for the virtual source on the view of the distortion of the finite-amplitude wave," J. Acoust. Soc. Jpn. **44**, pp.669-672 (1988). [*in japanese*]

10) T.Tsuchiya, Y.Watanabe and Y.Urabe; "Measurements of non-interacting angle in the scattering of sound by sound for gases," Jpn. J. Appl. Phys. Suppl. **27-1**, pp.73-75 (1988).

11) P.J.Westervelt; "Parametric acoustic array," J. Acoust. Soc. Am. **35**, pp.535-537 (1963).

12) T.Tsuchiya and Y.Kagawa; "Finite element analysis of focusing field in nonlinear acoustic waves," Jpn. J. Appl. Phys. Suppl. **30-1** (1991) to appear.

13) T.Tatsumi; "Fluid dynamics," Baifu-kan, Tokyo (1982). [*in japanese*]

14) O.C.Zienkiewicz: "The finite element method," McGraw-Hill (1977).

15) H.Mitome; "An exact solution for finite-amplitude plane sound waves on a dissipative fluid," J. Acoust. Soc. Am. **86**, pp2334-2338 (1989).